# Mapping the Cavitation Intensity in an Ultrasonic Bath Using The Acoustic Emission

**Vijayanand S. Moholkar, Shishir P. Sable, and Aniruddha B. Pandit**
Dept. of Chemical Engineering, University Dept. of Chemical Technology, University of Bombay, Bombay—400 019, India

*A new method for separate identification and determination of the spatial distribution of the two components of the energy intensity in an ultrasound bath (due to the ultrasound waves and cavitation activity) uses two media—cavitating (water) and noncavitating (silicon oil)—under the conditions of the acoustic field in the ultrasound bath. The variation of cavitation intensity in the frequency domain was obtained by subtracting the acoustic emission spectrum of silicon oil from that of water. Measurements at various locations in the bath revealed significant spatial variations in the cavitation intensity in the bath. The local cavitation phenomena in the bath (stable or transient cavitation) were explained based on the spectral characteristics of acoustic emission. The radial dynamics of the bubbles at the location of cavitation intensity measurements was determined using the Gilmore model of bubble dynamics. The bubbles in the region of highest cavitation intensity underwent a transient motion, while the bubbles in the region of lowest cavitation intensity underwent stable/oscillatory motion. The transient collapse of the bubbles that gives rise to local temperature and pressure maxima is at the root of the observed effects of ultrasound on chemical systems. The more violent the collapse of the bubbles, the higher the local cavitation intensity. It was verified using the spectral characteristics of the acoustic emission and simulation of the radial motion of the bubbles.*

## Introduction

The use of ultrasound for chemical synthesis is a highly active research area. Ultrasound makes available a range of energies on time scales that are not available from any other source. It affects both the homogeneous and heterogeneous chemical systems in several ways. It can accelerate a chemical reaction and allows less severe forcing conditions; cruder chemicals can be used for the synthesis than in the expensive purer versions, the number of steps in a multistep chemical synthesis can be reduced; or in some cases, it can completely switch the reaction pathway.

The basic underlying phenomenon behind the effects of ultrasound, whether physical, chemical, or biological, is *cavitation.* The word cavitation refers to the formation, growth, and collapse of vapor or gas bubbles under the influence of ultrasound. Depending on the frequency and intensity of the ultrasound waves, the bubbles can undergo either a stable, oscillatory motion for several acoustic cycles or a transient motion comprising a single growth and collapse phase in one or two acoustic cycles. On collapse, the transient cavitation bubbles produce very high temperatures and pressures, which are responsible for all the observed effects of ultrasound, such as erosion, sonoluminescence, and the effects on chemical systems just listed. Theoretical calculations report temperatures up to 5000°C and pressures up to 500 atm produced after the collapse of the cavitation bubbles.

Despite its efficacy on laboratory-scale processes, the interests of the chemical industry are not served by ultrasound technology. Three major factors have contributed to this. First, cavitation, which is paramount to all sonochemical reactions occurs only very near the surface of the sonicator and thus severely limits the volume of the *active* sonochemical

Correspondence concerning this article should be addressed to V. S. Moholkar.
Present address of V. S. Moholkar: Technology of Structured Materials (Textile Technology) Group, Department of Chemical Engineering, University of Twente, P.O. Box 217, 7500 AE Enschede, The Netherlands.

reactor. The second problem is the inability to obtain the desirable and uniform volumetric energy density at optimum cavitational conditions in the bulk volume of the reactor. This is attributed to both the current state of transducer technology and the attenuation of the acoustic field by cavitation at the sonicator surface. The third problem is the erosion of the sonicator surfaces at the high power intensities that are required for larger-scale reactors suitable for industrial-scale operations.

In the present work we address the second of the three problems just stated. Our aim in this work is to develop a new technique for finding the distribution of the cavitation intensity in an ultrasound bath. The energy intensity at a particular location in the ultrasound bath comprises two components: the energy intensity due to the ultrasound itself, and the cavitation intensity due to the local cavitation activity (that is, the oscillation and collapse of the bubbles, and the temperature and pressure pulses resulting from them). The second component of the total energy intensity (that is, cavitation intensity) contributes mostly to all the observed effects of cavitation. Attempts to map the energy dissipation pattern in an ultrasound bath have been made in the past. Ratoarinoro et al. (1995) have measured the bulk power dissipation in an ultrasound bath using calorimetric measurements. Contamine et al. (1994) have made attempts to distinguish between the physical and chemical effects of ultrasound using thermochemical and electrochemical probes. In a recent paper, Romdhane et al. (1997) measured the attenuation of ultrasound waves in a chemical reactor using a thermoelectric probe. Martin and Law (1980, 1983) have suggested the use of thermister probes for ultrasound intensity distributions in an ultrasound bath. Dahnke and Keil (1998a, b, 1999) and Dahnke et al. (1999a,b) have reported simulations of the 3-dimensional pressure fields in ultrasonic reactors of different geometries using the Helmholtz and Kirchhoff integral equation with homogeneous and inhomogeneous distribution of the cavitation bubbles. In their model, Dahnke and Keil (1998a,b, 1999) use the modified wave equation of Prosperetti and Commander (1989), which takes into account the effect of small-amplitude sinusoidal oscillations of the gas bubbles present in the liquid on the propagation of the pressure waves. Despite its rigorousness, the practical utility of the model of Dahnke and Keil (1998a,b, 1999) in the design of the ultrasound reactors is limited for several reasons. The homogeneous density distribution of the bubbles, as assumed by Dahnke and Keil (1998a,b, 1999), is difficult to achieve even in a well-stirred ultrasound bath. In addition, bulk movement of the liquid in the bath due to stirring can disturb the pressure field due to the scattering of ultrasound waves. In the simulation of the pressure fields with inhomogeneous distribution of the bubbles, Dahnke and Keil (1998a,b, 1999) divide the space between the ultrasound source and the opposite boundary in several planes, with the assumption that the gas-volume fraction varies in these planes. However, the gas-volume fraction in one particular plane is assumed to be homogeneous in these simulations. This assumption is not valid in practical cases, since the local bubble-volume fraction at any point in the bath changes continuously with the propagation of the ultrasound wave and does not remain homogeneous even for all points in one plane as assumed by Dahnke and Keil (1998a,b, 1999). In addition, the assumption that the bubble has a small-amplitude sinusoidal motion in the modified wave equation (Prosperetti and Commander, 1989) used by Dahnke and Keil (1998a,b, 1999) loses validity in the case of pressure waves with high amplitudes ( $> 1$ atm), where the bubble undergoes large-amplitude nonlinear motion.

This work is aimed at identifying the two components of the energy intensity in an ultrasound bath separately, using an experimental approach and treating the bubble as a secondary sound source. This novel technique uses two media for the propagation of ultrasound in the bath, one undergoing cavitation and the other noncavitating under the conditions of the frequency and intensity of the ultrasound bath. The spectral characteristics of the acoustic emission in these two media have been used to outline the spatial distribution of the cavitation intensity in the bath.

## Experimental

### *Experimental system*

Experiments were carried out in a stainless-steel low-powered ultrasonic cleaning bath (Dakshin Ltd., Bombay, India). The internal dimensions of the bath were: length = 0.15 m, breadth = 0.15 m, height = 0.15 m. Thus the bath had a surface area of 0.0225 $m^2$. The bath was scaled in *x-y-z* directions, with one of its bottom corners chosen as the origin of the coordinate system. The average amplitude of sound waves in the bath was calculated using the power rating of the bath (120 W) and the exposed area (0.0225 $m^2$). Nine random locations in the bath were chosen for the measurement of the acoustic intensity in the bath. The *x*- and *y*-coordinates of these locations were noted. A hydrophone (Bruel and Kjaer Ltd., Denmark, Type 8103) and a charge amplifier were used to measure the pressures at various locations in the bath. The distance between the hydrophone and the bottom of the bath was fixed at 5 mm. This value is based on measurements carried out by Chivate and Pandit (1993). Provision was made to hold the hydrophone at a fixed location and height in the bath. The bath was operated at 22 kHz after being filled with 300 mL of the medium. The output of the amplifier (the voltage it develops as a function of the pressure sensed by the hydrophone) was fed to the oscilloscope (LeCroy Ltd., Model 9310M). This oscilloscope had the facility of calculating the FFT of the input signal on-line.

### *Choice of the media*

Most literature on sonochemistry reports the employment of water as a medium for the experiments. The main reason for this is the poor response of organic liquids to ultrasound. The high vapor pressures of organic solvents prevent the transient collapse of the cavitation bubble, which is responsible for the observed cavitation effects. For the given conditions of ultrasound intensity and frequency, different solvents are characterized as cavitating or noncavitating based on the cavitation threshold for that solvent. The *cavitation threshold* is defined as the minimum pressure amplitude of the ultrasound waves required for the inception and continuance of cavitation. It is a function of the physical properties of the medium as well as the characteristics of the ultrasound pressure field (viz., frequency and intensity of the ultrasound

waves) in the bath. In the present work, two types of media were used, one with its cavitation threshold below the average pressure amplitude of the ultrasound pressure waves in the bath, and the other with its cavitation threshold above the average amplitude of the ultrasound pressure waves in the bath.

The average pressure amplitude of the ultrasound waves in the bath was found to be 1.248 atm, based on the power rating and the area of the bottom of the bath, though it varies spatially due to the conical divergence of the ultrasound waves originating from the transducer, as mentioned by Martin and Ward (1992). Since the cavitation threshold for water, the most widely used medium, is below the average amplitude of the ultrasound waves in the bath (approx. 0.6 atm for aerated water and 1.2 atm. for deaerated water), the first cavitating medium out of the two used in this work was fixed as water. The second medium, which has to be noncavitating under the conditions present in the bath, was fixed as silicon oil [cavitation threshold = 3.9 atm, Mason (1988)].

### *Experimental procedure*

As mentioned earlier, the bath was scaled in three directions, and nine locations were chosen for pressure measurement. In order to achieve consistency in the results, the volume of the medium in the bath was kept constant at 300 mL for all measurements. To avoid any rise in the temperature in the bath during the experiments, the bath was operated intermittently, with pressure pulses of short duration. The temperature of the medium during the experiments was 25°C. Prior to the measurements, silicon oil was heated to 180°C to remove any water impurities, if present. In addition, the silicon oil was degassed by pulling a vacuum over it to remove any nuclei for cavitation in the form of dissolved gas. Water was allowed to stand undisturbed in the bath for at least 2 h before the measurements to avoid interference from large bubbles (with radii $>$ 50 $\mu$m). The duration of the pulse recorded by the hydrophone was fixed at 500 $\mu$s (which corresponds to approximately 10 acoustic cycles). Since the phenomenon of cavity oscillation and collapse is of a completely random nature, two consecutive runs of the same duration may yield completely different results. Therefore, 50 pressure pulses were collected and analyzed at every location to average out this effect. The FFT of the pressure pulse was obtained on the oscilloscope and the absolute magnitudes of the Fourier coefficients for frequencies from 2 to 250 kHz were written down. This frequency range was selected based on the frequency-response curve of the hydrophone supplied by the manufacturers. This procedure was carried out using water as the medium in the first part and the silicon oil as medium in the second part of the experiments. The data collected from the experiments were analyzed using Math Cad software (version 8.0).

### *Method of analysis*

The pressure pulses collected at the same location with water and silicon oil as cavitation media are of a different character. The pressure pulse sensed by the hydrophone with water as the medium comprises pressure due to the ultrasound waves with the pressure pulses caused by the oscillations/transient collapse of the bubbles superimposed over it, while the pressure pulse in the case of silicon oil comprises only the pressure due to the ultrasound waves, since it does not undergo cavitation in the ultrasound bath. The pressure pulses arising from the transient collapse of an individual bubble undergo large attenuation due to absorption by the bubble cloud surrounding the collapsing bubble and nonlinearities of the medium. Matula et al. (1995) have estimated the attenuation of the pressure pulse for bubbles as being greater than 5 $\mu$m, using a generalized form of the Burger's equation. Calculations by Matula et al. (1995) show that the measured amplitude of the pressure pulse is almost 1000 times lower than its actual value at a distance as low as 1 mm from the center of the bubble generating the pressure pulse, if we assume that the pressure pulses resulting from the transient collapse of the bubbles are affected by spherical spreading. Therefore, there is a large difference between the magnitude of the pressure pulses theoretically calculated and those actually measured. Similarly, the ultrasound waves also undergo severe attenuation as they travel through a highly viscous medium like silicon oil. The estimation of the attenuation coefficient for the two media used in the experiments is explained in the next section.

The data obtained from the experiments is composed of a series of frequencies and corresponding Fourier coefficients at various locations in the bath. To average out the cavitation effect, an average acoustic-emission spectrum was obtained by averaging the values of the Fourier coefficients for the frequency range under consideration in the FFT of the 50 pressure pulses for both water and the silicon oil as the propagation media for ultrasound. To accurately estimate the amplitude of the ultrasound pressure, the Fourier coefficients for the silicon oil for the frequency range under consideration were corrected, taking into consideration the damping coefficient for the ultrasound waves. The Fourier coefficients for various frequencies in the average acoustic-emission spectrum with silicon oil as medium were subtracted from the Fourier coefficients for the corresponding frequencies in the average acoustic-emission spectrum with water as the medium. The resulting spectrum represents the variation of cavitation intensity alone at a particular location in the ultrasound bath in the frequency domain. The inverse FFT of this spectrum was then obtained to get the variation of the cavitation intensity at a particular point in the time domain (please note that only the real part of the inverse FFT represents the variation of the cavitation intensity in the time domain.)

## Propagation of the Ultrasound Waves, Bubble Dynamics, and Analysis of Acoustic-Emission Spectra

### *Attenuation of the acoustic waves*

One of the cavitation media used in the current work, water, is expected to have a large number of nuclei, that is, cavitation generating spots. These locations could be small bubbles already present or arising from collapsed cavitation bubbles, or they could be gas trapped in the crevices of the reactor wall. When the liquid is subjected to ultrasound, these nuclei respond differently, depending on their initial sizes and the amplitude and frequency of the sonic field. During prop-

agation of the ultrasound waves in the medium, the intensity of the sound wave decreases with the distance from the emitter surface. This attenuation is a result of several factors, such as reflection, refraction, or scattering of the sound, and most importantly, conversion of the kinetic energy of the wave into heat. Attenuation of the ultrasound is a function of the density and viscosity of the medium. The attenuation or damping coefficient is given as

$$\alpha_s = \frac{8\mu\pi^2 f^2}{3\rho C^3}, \tag{1}$$

where $\mu$ is the viscosity and $\rho$ is the density of the medium; and $f$ and $C$ are the frequency and velocity of the sound, respectively. Substituting properties of water ( $\mu = 10$ cP, $\rho =$ 1,000 kg/m$^3$, $C = 1481$ m/s), the damping coefficient for water is estimated as $3.92\times10^{-6}$ m$^{-1}$. In a similar way the damping coefficient for silicon oil is calculated from its physical properties ( $\mu = 6.3$ P, $\rho = 969$ kg/m$^3$, $C = 1472$ m/s) as $2.59\times10^{-4}$ m$^{-1}$.

### *Bubble dynamics*

Simulations of the sound radiation from the bubble field have been reported by Cramer and Lauterborn (1981), Ilyichev et al. (1989), Grossman et al. (1997), and Hilgenfeldt et al. (1998). The bubble models introduced so far cannot handle bubble fields with thousands of bubbles with strong interactions between them. Even with this difficulty, Ilyichev et al. (1989) have proved that all characteristic features of the acoustic emission spectra are explained by the dynamic behavior of a single bubble. The far-field sound pressure at a distance $r \gg R$ from the center of the bubble can be calculated as,

$$P_s(r,t) = \frac{\rho}{4\pi r}\frac{d^2V_b}{dt^2} = \rho\frac{R}{r}\left[2U^2 + R\frac{dU}{dt}\right], \tag{2}$$

where $V_b$ is the volume of the bubble, $R$ is the radius of the bubble, $U$ and $dU/dt$ are the first and second derivatives of the bubble radius corresponding to the velocity and acceleration of the bubble radius; $\rho$ is the density of the medium; and $r$ is the distance from the bubble center.

The radial motion of a bubble can be described by the bubble dynamics equation. The dynamic behavior of the cavity was first studied by Rayleigh (1917). He proposed an equation for the dynamics of the bubble, which was later modified by Plesset (1949), who included the viscous and surface-tension effects. Various modified versions of the Rayleigh-Plesset equation have appeared in the last few decades, for example, Keller and Miksis (1980), Gilmore (1952), and Prosperetti et al. (1986). However, a detailed comparison of the solutions obtained from these equations [Lastman and Wentzell (1981), Lohse (personal communication, 1998)] shows that significant deviations in the solutions occur only for bubbles driven at very high-pressure amplitudes ( $\geq 5$ atm) and that have large radii.

For our work, we chose the Gilmore equation based on the Kirkwood-Bethe hypothesis (1948), which states that the shock waves due to bubble motion are propagated with a velocity equal to the sum of the sound velocity and fluid velocity [Akulichev (1971)]. According to this equation, the radial motion of the bubble is described by

$$R\left(1-\frac{U}{C}\right)\frac{d^2R}{dt^2} + \frac{3}{2}\left(1-\frac{U}{3C}\right)\left(\frac{dR}{dt}\right)^2 - \left(1+\frac{U}{C}\right)H - \frac{U}{C}\left(1-\frac{U}{C}\right)R\frac{dH}{dR} = 0, \tag{3}$$

where $C$ is the local velocity of sound, and $H$ is the free enthalpy on the surface of the bubble, and is given as

$$H(P) = \int_{P_\infty}^{P(R)}\frac{dP}{\rho}, \tag{4}$$

where $P(R)$ is the pressure in the bulk liquid just outside the bubble boundary, and $P_\infty$ is the pressure in the bulk liquid away from the bubble. We substitute the following expressions in the preceding equation for $P(R)$ and $P_\infty$:

$$P(R) = \left(P_o + \frac{2\sigma}{R_o} - P_v\right)\left(\frac{R_o}{R}\right)^{3\gamma} - \frac{2\sigma}{R} \tag{5}$$

$$P_\infty = P_o - P_A\sin(2\pi ft), \tag{6}$$

where $P_o$ is the ambient (in present case atmospheric) pressure; and $P_A$ is the amplitude and $f$ is the frequency of the ultrasound waves. The various physical properties of the media are represented by $\rho$ (density), $\sigma$ (surface tension), and $P_V$ (vapor pressure). $R_o$ is the initial radius of the bubble; $\rho_o$ is the density in the undisturbed state; and $\gamma$ is the polytropic constant. Naidu et al. (1994) have assumed the bubble motion to be a combination of isothermal ($\gamma = 1$) and adiabatic ($\gamma = C_p/C_v$) behavior. They assume that the transition from isothermal to adiabatic phase occurs when, in the collapse phase, the partial pressure of the gas in the bubble becomes equal to the vapor pressure of the liquid, as per Flynn's hypothesis (Flynn, 1964). Plesset and Prosperetti (1977) have shown that the thermal behavior of the bubble depends on the (thermal) Péclet number $Pé = (R_0^2\omega)/\kappa$ and thermal diffusion length $\sqrt{\kappa/\omega}$, where $\kappa$ is the thermal diffusivity of the bubble contents (which is a mixture of air and water vapor in the present case), and $\omega$ is the angular frequency. Hilgenfeldt et al. (1996) propose that since the bubble dynamics equation contains time scales much smaller than $\omega^{-1}$, the frequency $\omega$ in the calculation of $Pé$ should be replaced by $|U|/R$. This replacement leads to a value of $Pé$ that is as large as $10^4$ at the instants of rapid bubble-wall movement, which implies that the bubble motion is adiabatic. However, the condition for which $Pé \gg 1$ lasts for only very short time intervals $\approx 1$ ns. Therefore Hilgenfeldt et al. (1996) propose that the global dynamics of the bubble are not affected by setting the polytropic exponent ($\gamma$) equal to one uniformly in time, thus parametrizing the isothermal conditions at the bubble wall, induced by the large heat capacity of water. Based on this hypothesis of Hilgenfeldt et al. (1996), the mo-

tion of the bubble has been assumed to be isothermal in the present case.

$P$ can be expressed from the equation of state for water in the form:

$$P = A\left(\frac{\rho}{\rho_o}\right)^n - B, \tag{7}$$

where $A$, $B$, and $n$ are constants. The water values of these constants are $A = 3001$ atm, $B = 3000$ atm, and $n = 7$ (Akulichev, 1971). Now after integration of Eq. 4 using Eqs. 5, 6, and 7, we obtain the free enthalpy of the bubble surface as

$$H = \frac{n}{n-1}\frac{A^{1/n}}{\rho_o}\left\{\left[\left(P_o + \frac{2\sigma}{R_o}\right)\left(\frac{R_o}{R}\right)^{3\gamma} - \frac{2\sigma}{R} + B\right]^{(n-1)/n} - \left[P_o - P_A \sin \omega t + B\right]^{(n-1)/n}\right\}. \tag{8}$$

In the equation $C$ is the local velocity of the liquid and is expressed as $(\partial P/\partial \rho)^{1/2}$. Using Eqs. 4 and 7, it is calculated as

$$C = \left[C_o^2 + (n-1)H\right]^{1/2}, \tag{9}$$

where $C_o$ is the velocity of liquid at standard temperature and pressure (STP) conditions and is given as $C_o = \sqrt{An/\rho_o}$.

As stated earlier, the sound waves originating from the bubble undergo severe attenuation due to their spherical divergence. Therefore, parameter $r$ in Eq. 2 is fixed as 1 mm. Using the Runge-Kutta fourth-order method with adaptive time step-size control (Press et al., 1992), the initial conditions for the numerical solution of Eq. 3 are $t = 0$, $R = R_o$, and $U = 0$. The simulations are stopped at the end of the first compression phase in the radial motion of the bubble (after $t > 0$), in which the Mach number of the bubble wall $|U/C|$ exceeds 1 (Gaitan et al. 1992).

Cavitation bubbles are classified as stable or transient according to their radial motion under the influence of the acoustic field. Flynn (1975) has characterized the stable and transient cavities depending on their expression in the radial motion. He hypothesized that for a bubble to undergo transient collapse, the ratio $R_{max}/R_o$ during the radial motion of the bubble should exceed the minimum value given by

$$\frac{R_{\max}}{R_o} = \left(\frac{7.48\ P_{go}}{P_o}\right)^{1/3}, \tag{10}$$

where $P_{go}$ is the initial gas pressure in the bubble. For air bubbles in water this ratio is approximately 2. Above this ratio, the dynamic behavior of a cavitation bubble is controlled by the inertial forces in the liquid surrounding it. Above this critical value, the liquid transfers an ever increasing amount of energy to the collapsing bubble with an increasing value of ratio $R_{max}/R_o$, and hence the collapse is more and more violent, giving rise to pressure pulses of higher and higher magnitude. The relation between the dynamic behavior of the bubbles and the acoustic-emission spectra is explained in the next section.

### *Analysis of the acoustic-emission spectrum*

One of the principal tasks in cavitation research is the experimental study and theoretical interpretation of the acoustic-emission spectrum. Many attempts have been made to explain the spectrum of acoustic cavitation noise, but complete insight has not been obtained. Young (1989) and Leighton (1994) have given detailed explanations of the acoustic emission by the cavitation bubbles under two distinct cavitation regimes: stable cavitation and transient cavitation. It is generally known that an acoustic cavitation noise spectrum consists of various peaks closely related to the frequency of the driving field ($f$). These peaks correspond to the driving ultrasound frequency and its harmonics ($nf$, $n = 2, 3, 4, \ldots$) and subharmonics ($f/m$, $m = 2, 3, 4, \ldots$). The first subharmonic ($f/2$) was observed by Esche (1952), who also reported the $f/3$ subharmonic. Subsequently, Bohn (1957) reported the $f/4$ subharmonic. The harmonics $nf$ are explained in terms of forced nonlinear bubble oscillations, and the noise background is explained in terms of the shock waves emitted by the collapsing bubbles. The first detailed explanations of the subharmonics, which were later confirmed by Neppiras (1969a,b) and Eller and Flynn (1969), were given by Guth (1956). Guth (1956) demonstrated that a bubble with an equilibrium radius greater than the resonance value would pulsate, and as a consequence would radiate the subharmonic frequencies. Numerical calculations based on the Noltingk–Neppiras model [Lauterborn (1970, 1976) and Prosperetti (1975)] showed that the pulsations of a bubble excited at an ultraharmonic resonance frequency can also be a source of the subharmonic frequencies in the acoustic-emission spectra. Akulichev (1967) found still another possible reason for the presence of the subharmonic components in the acoustic-emission spectrum. He demonstrated that because of the inertial forces (when the pressure amplitude of the exciting field considerably exceeds the threshold) a bubble expands even during the compression half-period and passes the contraction phase. As a result, the time period of the pulsation of the bubble becomes a multiple of the period of the exciting field and the subharmonic components appear in the noise spectrum of the bubble sound emission.

At very low intensities, the acoustic-emission spectrum is composed of the fundamental frequency only. With a slow rise in intensity, but still below the transient threshold, the larger bubbles start oscillating nonlinearly. At this intensity the acoustic-emission spectrum comprises the peaks corresponding to the driving frequency and its harmonics, with the second-order harmonic being most prominent. These harmonics may also correspond to the nonlinearity of the medium, but in a gassier liquid the contribution to the harmonics is mainly due to the bubbles.

In a stable cavitation field, the subharmonic signals are weak. The two major explanations for this are as follows:

1. The surface vibrations of the bubbles are not very strong at low sound intensities. These are pure distortion modes not involving any area change and are therefore weakly coupled

**Table 1. Threshold Pressure Amplitudes for Subharmonic Emission for Bubbles of Different Sizes**

| $R_o$ ($\mu$m) | $\omega_r$ (kHz) | $P_T$ (atm) |
|---|---|---|
| 2 | 1,980 | $6.429\times10^9$ |
| 4 | 900 | $1.768\times10^9$ |
| 6 | 578 | $8\times10^8$ |
| 8 | 425 | $4.68\times10^8$ |
| 10 | 336 | $3.031\times10^8$ |

to the liquid. Therefore these are not easily detected by the hydrophones.

2. As stated earlier, the subharmonic signal was explained by Guth (1956) as being due to the bubbles of twice the resonance size for the driving frequency being excited. Eller and Flynn (1969), Safar (1970), and Nayeh and Saric (1974) have given different expressions for the threshold of such an emission. Here we use the expression for this threshold given by Eller and Flynn (1969),

$$P_T = 6P_o\left[\left(\frac{\omega}{\omega_r}-2\right)^2+\delta^2\right]^{1/2}, \tag{11}$$

where $\delta$ is the total damping coefficient for the radial motion of the bubble, and is given as

$$\delta = \frac{b}{\omega_r m}, \tag{12}$$

where $b$ is the total damping constant, $\omega$ and $\omega_r$ are angular frequency of the driving acoustic field and the resonance angular frequency of the bubble, respectively, and $m$ is the mass of the bubble contents (here we assume it to be gas alone). The resonance frequency of a bubble is given as,

$$\omega_r^2 = \left(\frac{1}{\rho_L R_o^2}\right)\left[3\gamma P_o - \frac{2\sigma}{R_o}\right]. \tag{13}$$

Table 1 summarizes the subharmonic emission pressure thresholds for some typical bubble sizes. From Table 1 it can be inferred that under the ultrasound frequency and intensity conditions in the current experiments such an emission is not possible.

A significant change occurs in the acoustic-emission spectrum when the transient cavitation starts: there is a sudden increase in the intensity of all the harmonics and subharmonics. Many researchers have recorded and discussed these emissions [Lauterborn (1970, 1976), Neppiras (1969a,b, 1980)]. The subharmonic emission may be generated by a prolonged expansion phase and a delayed collapse phase, which can occur during transient cavitation. As stated earlier, Akulichev (1967) demonstrated how as a result of the inertial forces a bubble could continue to expand even after the rarefaction half-period of the acoustic cycle (during the compressive half-period). Similarly, Apfel (1981) pointed out that the transient cavitation can be characterized by the bubbles that survive for more than one acoustic cycle and repeat the form of radial motion as in the first cycle. This type of motion can generate the subharmonic emission. Neppiras (1980) also suggested that a form of periodic unstable oscillation of a bubble driven at twice its resonance frequency near the threshold might emit subharmonic frequencies. This is now regarded as the best available threshold indicator for transient cavitation. However, Walton and Reynolds (1984) stated that transient cavitation is characterized by a continuum in the sound spectrum.

## Results and Discussion

As stated earlier, the energy intensity in an ultrasound bath is composed of two components:

1. The energy intensity of the ultrasound waves.
2. The cavitation intensity due to the dynamic behavior of the bubbles under the influence of ultrasound, which gives rise to the local high temperatures and pressures.

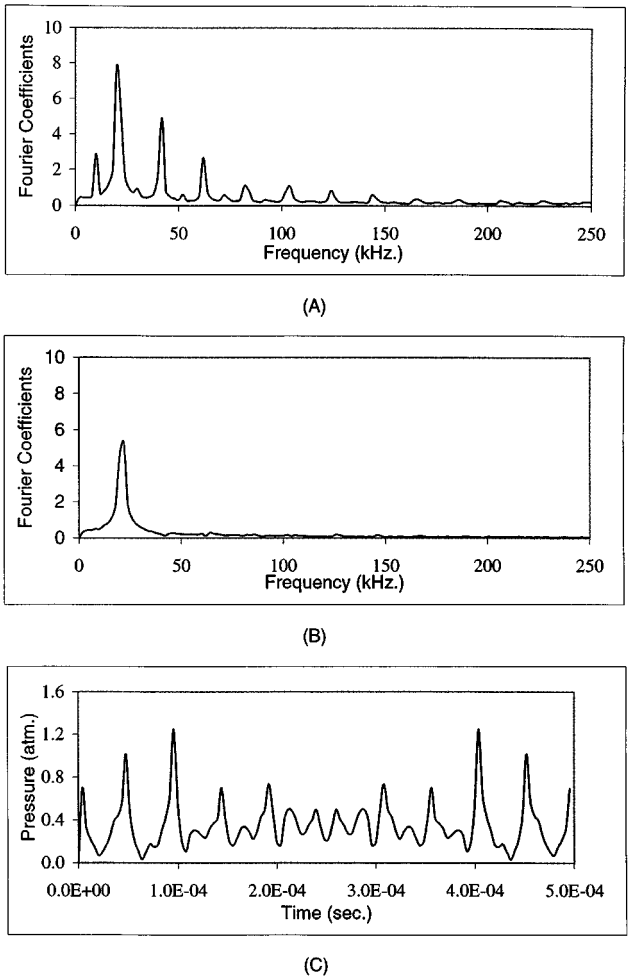


**Figure 1. (A) Average acoustic emission spectrum at location [3.5, 7.3] with water as medium; (B) average acoustic emission spectrum at location [3.5, 7.3] with silicon oil as the medium; (C) time variation of the cavitation intensity at location [3.5, 7.3].**

**Table 2. Fourier Coefficients in the Acoustic Emission Spectrum at Location [3.5, 7.3]**

| Frequency (kHz) | with Water | with Silicon Oil |
|---|---|---|
| 11 | 2.89 | 0.46 |
| 1st Subharmonics, $f/2$ | | |
| 22 | 7.81 | 5.33 |
| (Fundamental, $f$) | | |
| 44 | 4.89 | 0.14 |
| 1st Harmonic, $2f$ | | |
| 66 | 2.67 | 0.11 |
| 2nd Harmonic, $3f$ | | |
| 88 | 1.12 | 0.10 |
| 3rd Harmonic, $4f$ | | |
| 110 | 1.09 | 0.096 |
| 4th Harmonic, $5f$ | | |
| 132 | 0.84 | 0.09 |
| 5th Harmonic, $6f$ | | |

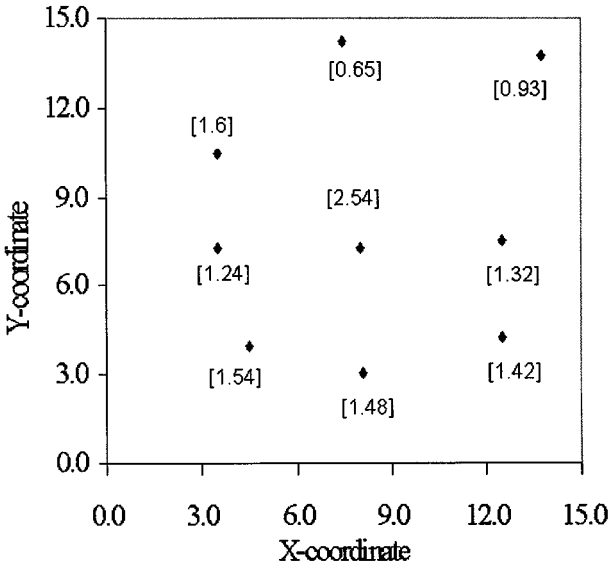


**Figure 2. Top view of the ultrasonic bath showing locations of the acoustic emission measurements and the amplitude of the cavitation intensity at these locations.**

*X* and *Y* coordinates show length and breadth of the bath in cm; the figures given in square brackets denote the amplitude of the cavitation intensity in atmospheres.

The use of two different media for the ultrasound propagation enables us to identify these two components separately. The acoustic emission spectrum with water as the medium is composed of the pressure due to the ultrasound waves, with the pressure pulses due to bubble oscillation/collapse superimposed on it. Conversely, cavitation does not occur in the silicon oil for the conditions of the ultrasonic pressure field in the bath, since the amplitude of the ultrasound waves in the bath is below the cavitation threshold for silicon oil. Therefore the acoustic emission spectrum with water as the medium comprises the fundamental (driving) frequency and its harmonics and subharmonics, while the acoustic emission spectrum with the silicon oil as the medium comprises only the peak corresponding to the fundamental frequency. This is evident from Figure 1A and 1B, which show the acoustic-emission spectra with water and silicon oil as media, respectively, at a particular location (coordinates [3.5, 7.3]) in the bath. Figure 1C shows the inverse FFT of the difference between the acoustic-emission spectrum with water and silicon oil as the media, that is, time variation of the cavitation intensity obtained from the procedure described before. It can be seen that the amplitude of the cavitation intensity at this location is 1.24 atm. The Fourier coefficients for the fundamental frequency, its first subharmonic ( $f/m$, $m = 2$), and five harmonics ($nf$, $n = 2, 3, \ldots, 6$) in Figures 1A and 1B are given in Table 2. It can be inferred from Table 2 that in the acoustic emission spectrum with silicon oil (Figure 1B), the Fourier coefficient corresponding to the fundamental frequency is the most prominent and the Fourier coefficients of all other frequencies (corresponding to subharmonic and harmonics) are negligible. Contrary to this, in the acoustic emission spectrum with water (Figure 1A), the magnitudes of the Fourier coefficient of the subharmonic and harmonics of the fundamental frequency are significant, and the magnitude of the Fourier coefficients of the harmonics decreases with the increasing order of the harmonics. A comparison of the magnitudes of the corresponding Fourier coefficients in the acoustic-emission spectra with water and silicon oil as media reveals a significant discrepancy, which is representative of the cavitation events. Therefore the method of subtracting the Fourier coefficients in the acoustic-emission spectrum with oil from the corresponding coefficients in the acoustic-emission spectrum in water can give the information about cavitation events that occur in water but are absent in silicon oil due to its large cavitation threshold.

The locations of cavitation intensity measurement in the bath and the amplitude of the cavitation intensity at these locations are shown in Figure 2. The amplitude of the cavitation intensity at various locations is given between square brackets in atmospheres. It can be inferred from Figure 2 that the cavitation intensity is concentrated at the center of the bath, while it decreases considerably at the corners and edges of the bath. This can be attributed to the conical divergence of the acoustic waves in the bath generated by the transducer located at the bottom (Martin and Ward, 1992). Due to the conical divergence of the waves, the corners of the bath remain outside the insonated zone, and therefore the intensity of the ultrasound waves at these locations is quite low, resulting in low cavitation intensities.

The average acoustic-emission spectra at different locations in the bath with water as the medium show interesting features. At some locations the average acoustic-emission spectra show a strong subharmonic peak corresponding to the transient cavitation, while at some locations only the peaks corresponding to the fundamental frequency and its harmonic are present. This feature can be used to determine the cavitation intensity at a particular location and also to distinguish the zones of stable and transient cavitation, as discussed in sub section on the analysis of the acoustic-emission spectrum. Figure 3 shows the average acoustic emission spectra at locations of maximum (Figure 3A) and minimum (Figure 3B) and average cavitation intensity (Figure 3C). The major difference in the characteristics of the average acoustic-emission spectrum at the locations of minimum and maxi-

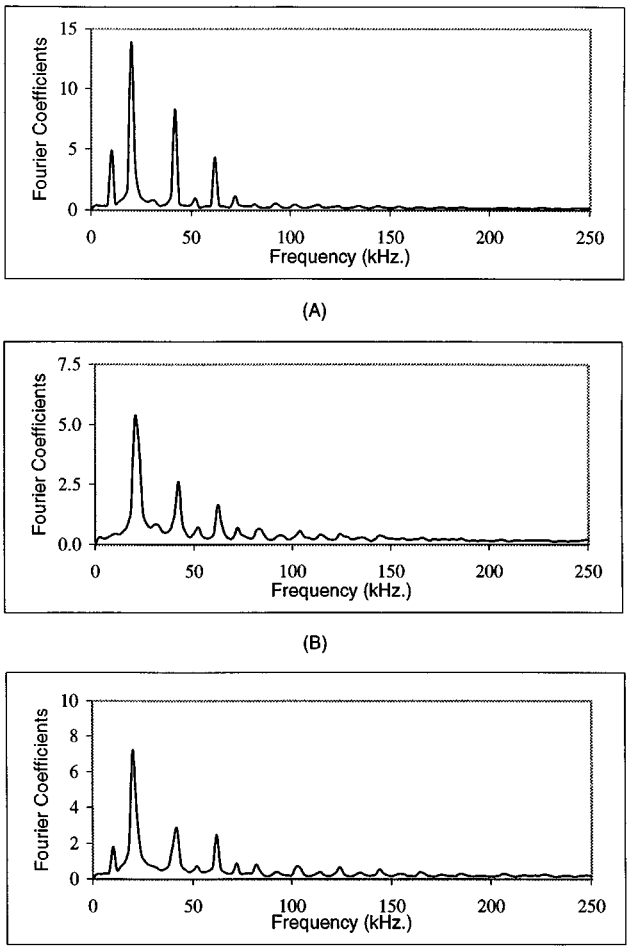


**Figure 3. Average acoustic emission spectrum in water: (A) at the location with the highest amplitude of the cavitation intensity (location coordinates [8, 7.3]); (B) with the lowest amplitude of the cavitation intensity (location coordinates [7.5, 12.5]); (C) with the average amplitude of the cavitation intensity (location coordinates [12.5, 7.5]).**

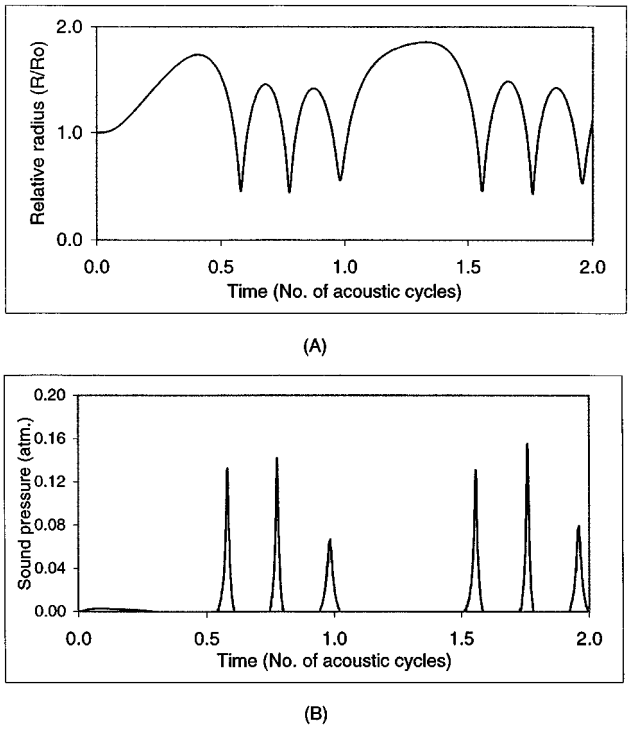


**Figure 4. Simulation of (A) radial motion of the bubble, and (B) sound emission from the bubble at location with minimum cavitation intensity (coordinates [7.5, 12.5]).**

Parameters for simulation; $R_o = 10$ $\mu$m, $\mu = 10$ cP, $\sigma = 0.072$ N·m, $P_A = 0.9$ atm, $f = 22$ kHz, $P_v = 3{,}168$ N·m$^{-2}$.

mum intensity is the presence of a subharmonic peak in the spectrum at the location of maximum cavitation intensity and its absence in the spectrum at the location of minimum cavitation intensity. In addition, the intensity of the harmonics relative to the fundamental frequency is also higher than that in the spectrum at the location of minimum cavitation intensity. In the average acoustic-emission spectrum at the location of the average cavitation intensity, though the subharmonic peak is present, its amplitude is less than the subharmonic peak in the average acoustic-emission spectrum at the location of the maximum cavitation intensity. As written earlier, due to the conical divergence of the acoustic waves, the ultrasound intensity at the corner falls below the transient threshold and bubbles at these locations do not undergo a transient collapse but a stable oscillatory radial motion. Typical bubble-size distribution in the bath is abut 2–10 $\mu$m. Figures 4, 5, and 6 show the radial motion of a bubble of size 10 $\mu$m and the acoustic emission from it at the locations of minimum, average, and maximum cavitation intensity, respectively, with water as the medium, using Eqs. 2 and 3. The amplitude of the driving pressure $P_\infty$ at these locations was determined from the acoustic-emission spectrum with silicon oil as the medium at that location after correction for the attenuation of the ultrasound waves in the silicon oil and water. The other parameters for simulation are shown in the figure captions. It can be seen that at location [8, 7.3], which has the maximum cavitation intensity, the bubble undergoes growth and collapse in two acoustic cycles representing the kind of radial motion given by Akulichev (1967) that is responsible for the subharmonic emission. On the other hand, at location [7.5, 12.5], which has the lowest cavitation intensity, the radial motion of the bubble is rather stable and oscillatory, typical of stable cavitation. In the region of average cavitation intensity (with location coordinates [12.5, 7.5]) the bubble undergoes a transient collapse after several oscillations, but the maximum radius reached during the motion is lower than that at the location of highest cavitation intensity. Analysis of the acoustic emission spectrum given in the subsection on the analysis of the acoustic-emission spectrum suggests that the presence of the subharmonic peak in the acoustic-emission spectrum is representative of the transient cavitation, or as pointed out by Akulichev (1967), a high energy stable cavitation where bubbles may survive for two or

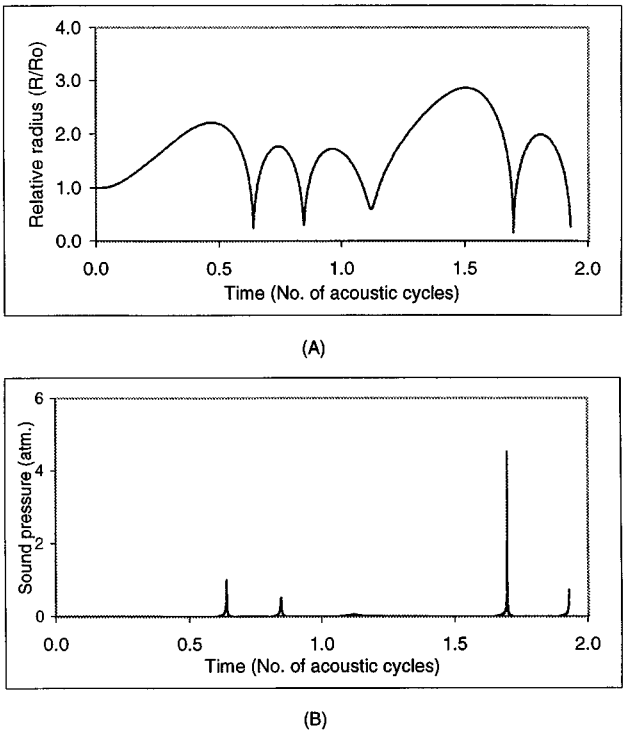


**Figure 5. Simulation of (A) radial motion of the bubble, and (B) sound emission from the bubble at a location with average cavitation intensity (coordinates [12.5, 7.5]).**

Parameters for simulation: $R_o = 10$ $\mu$m, $\mu = 10$ cP, $\sigma = 0.072$ N·m, $P_A = 1.12$ atm, $f = 22$ kHz, $P_v = 3{,}168$ N·m$^{-2}$.

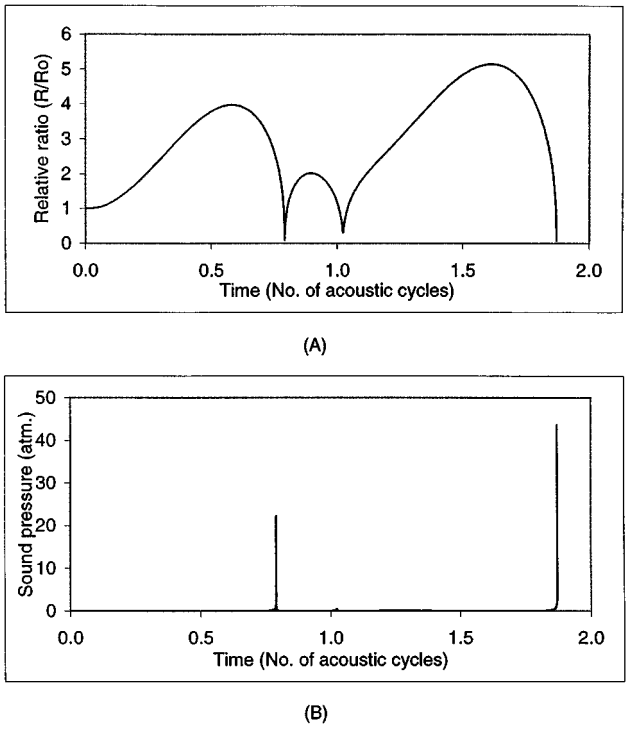


**Figure 6. Simulation of (A) radial motion of the bubble, and (B) sound emission from the bubble at location maximum cavitation intensity (coordinates [8, 7.3]).**

Parameters for simulation: $R_o = 10$ $\mu$m, $\mu = 10$ cP, $\sigma = 0.072$ N·m, $P_A = 1.85$ atm, $f = 22$ kHz, $P_v = 3{,}168$ N·m$^{-2}$.

three acoustic cycles before a transient collapse. According to this hypothesis, the bubbles at location [8, 7.3], with maximum cavitation intensity, should undergo transient motion, while bubbles at location [7.5, 12.5], with minimum cavitation intensity, undergo stable oscillatory motion. Simulation of the radial motion of the bubble and sound field produced by it at the locations of the minimum, maximum, and average cavitation intensities supports this conclusion. The difference between the amplitude of the subharmonic peak at locations of average and maximum cavitation intensity is explained by Flynn's hypothesis (Flynn, 1975) given in the subsection on bubble dynamics. The bubbles in the region of average cavitation intensity undergo a relatively less violent collapse than the bubbles in the region of the highest cavitation intensity due to their lower expansion. Therefore, the intensity of the subharmonic peak in the average acoustic-emission spectra at this location, which is representative of cavitation intensity, is also low.

## Conclusion

The present work introduces a novel method of determining the cavitation intensity by filtering the acoustic signal to separate the cavitation energy component in the acoustic-emission spectra in the ultrasonic bath. The characteristics of the acoustic-emission spectra (the presence of the subharmonic peak) at different locations in the bath and the dynamic behavior of the bubbles at these locations confirm the distribution of the cavitation intensity determined with this method. Experimentally measured local pressure amplitudes of ultrasound waves have been used for the simulations of the local bubble dynamics using the Gilmore model. Thus the approach proposed in this work gives information not only about the attenuated/modified pressure fields due to the presence of the cavitation bubbles, but also points out the contribution of the cavitation events in altering the pressure field, not only in terms of the attenuation and damping [approach of Dahnke and Keil (1998a,b, 1999)] but in treating the bubble as an additional sound-pressure source. The two components of the energy intensity in ultrasound bath—the acoustic intensity and the cavitation intensity—are interdependent. A reduction in the amplitude of the ultrasonic waves at the corner of the ultrasound bath causes a significant decrease in the cavitation intensity at that location. For an effective scale-up of the ultrasound reactor, it is of prime importance that the energy dissipation pattern in the reactor be known precisely. One of the major shortcomings of the ultrasound baths is the directional sensitivity of the ultrasound waves in the bath, which creates a nonhomogeneous energy dissipation pattern. Efforts are being made to overcome this problem by using tubular reactors with ultrasound intensity concentrated at the core of the reactor, but any industrial-scale operation is not reported as yet. The growth and transient collapse of the bubbles under the influence of ultrasound and the extremes of temperature and pressure pro-

duced thereby is at the center of all observed effects of ultrasound on chemical systems. Therefore, for an effective scale-up, along with the homogeneous distribution of the ultrasound waves, a precise knowledge of the spatial distribution of the cavitation intensity is of prime importance. The current work provides a technique based on the analysis of the acoustic-emission spectrum for the preceding objective. We expect this technique to contribute to the optimization of the ultrasound reactor for the production of a uniform energy dissipation pattern in it.

## Acknowledgment

One of the authors (A.B.P.) acknowledges the funding of the DST (Government of India) for the project. Another of the authors (V.S.M.) acknowledges the help of Dr. ir. Sander Rekveld and Ir. Michiel Huitema (Textile Technology Group, Department of Chemical Engineering, University of Twente) in the analysis of the data and in the preparation of the manuscript.

## Notation

$C_p$ = specific heat at constant pressure, $J^o \cdot C^{-1} \cdot kg^{-1}$
$C_v$ = specific heat at constant volume, $J^o \cdot C^{-1} \cdot kg^{-1}$
$P_s$ = pressure amplitude of sound emission from bubble, $N \cdot m^{-2}$
$R_{max}$ = Maximum radius reached in the radial motion of the bubble, m
$U$ = bubble wall velocity, $m \cdot s^{-1}$

## Literature Cited

Akulichev, V. A., "The Structure of Solutions of Equations Describing Pulsations of Cavitation Bubbles," in Russian, *Akusticheskii J.*, **13**, 533 (1967).
Akulichev, V. A., "Pulsations of Cavitation Voids," *High Intensity Ultrasonic Fields*, L. D. Rosenberg, ed., Plenum Press, New York, p. 205 (1971).
Apfel, R. E., *Methods in Experimental Physics*, Vol. 19, P. D. Edmonds, ed., Academic Press, New York (1981).
Bohn, L., "Acoustic Pressure Variation and the Spectrum in Oscillatory Cavitation," *Acustica*, **7**, 201 (1957).
Chivate, M. M., and A. B. Pandit, "Quantification of the Cavitation Intensity in Fluid Bulk," *Ultrason.-Sonochem.*, **2**, S19 (1995).
Contamine, F., F. Faid, A. M. Wilhelm, J. Berlan, H. Delmas, "Chemical Reactions Under Ultrasound: Discrimination of Physical and Chemical Effects," *Chem. Eng. Sci.*, **49**, 5865 (1994).
Cramer, E., and W. Lauterborn, "On the Dynamics and Acoustic Emission of Spherical Cavitation Bubbles in Sound Field," *Acustica*, **49**, 226 (1981).
Dahnke, S. W., and F. J. Keil, "Modeling of Linear Pressure Fields in Sonochemical Reactors Considering an Inhomogeneous Density Distribution of Cavitation Bubbles," *Chem. Eng. Sci.*, **54**, 2865 (1999).
Dahnke, S. W., K. M. Swamy, and F. J. Keil, "A Comparative Study on the Modeling of Sound Pressure Field Distributions in a Sonoreactor with Experimental Investigation," *Ultrason. Sonochem.*, **6**, 221 (1999a).
Dahnke, S. W., K. M. Swamy, and F. J. Keil, "Modeling of Three-Dimensional Pressure Fields in Sonochemical Reactors with an Inhomogeneous Density Distribution of Cavitation Bubbles. Comparison of Theoretical and Experimental Results," *Ultrason.-Sonochem.*, **6**, 31 (1999b).
Dahnke, S. W., and F. J. Keil, "Modeling of Three-Dimensional Linear Pressure Fields in Sonochemical Reactors with Homogeneous and Inhomogeneous Density Distributions of Cavitation Bubbles," *Ind. Eng. Chem. Res.*, **37**, 848 (1998a).
Dahnke, S. W., and F. J. Keil, "Modeling of Sound Fields in Liquids with a Nonhomogeneous Distribution of Cavitation Bubbles as a Basis for the Design of Sonochemical Reactors," *Chem. Eng. Technol.*, **21**, 873 (1998b).
Esche, R., "Untersuchung der Schwingungskavitation in Flussigkeiten," in German, *Acustica*, **2**, AB208 (1952).
Eller, A., and H. G. Flynn, "Generation of the Subharmonics of Order One Half by Bubbles in a Sound Field," *J. Acoust. Soc. Amer.*, **46**, 722 (1969).
Flynn, H. G., "Cavitation Dynamics I: Mathematical Formulation," *J. Acoust. Soc. Amer.*, **57**, 1379 (1975).
Flynn, H. G., "Physics of Acoustic Cavitation in Liquids," *Physical Acoustics*, Vol. 1B, W. P. Mason, ed., Academic Press, New York (1964).
Gaitan, D. F., L. A. Crum, R. A. Roy, and C. C. Church, "Sonoluminescence and Bubble Dynamics for a Single Stable Cavitation Bubble," *J. Acoust. Soc. Amer.*, **91**, 3166 (1992).
Gilmore, F. R., *Hydrodynamic Laboratory Report*, California Institute of Technology, Pasadena (1954).
Grossmann, S., S. Hilgenfeldt, M. Zomack, and D. Lohse, "Sound Radiation of 3 MHz Driven Gas Bubbles," *J. Acoust. Soc. Amer.*, **102**, 1223 (1997).
Guth, W., "Nichtlineare Schwingungen von Luftblassen in Wasser," (in German), *Acustica*, **6**, 532 (1956).
Hilgenfeldt, S., D. Lohse, and M. P. Brenner, "Phase Diagrams for Sonoluminescing Bubbles," *Phys. Fluids*, 2808 (1996).
Hilgenfeldt, S., D. Lohse, and M. Zomack, "Response of Bubbles to Diagnostic Ultrasound: A Unifying Theoretical Approach," *Eur. Phys. J.*, **4**, 247 (1998).
Ilyichev, V. I., V. L. Koretz, and N. P. Melnokov, "Spectral Characteristics of Acoustic Cavitation," *Ultrasonics*, **27**, 357 (1989).
Keller, J. B., and M. J. Miksis, "Bubble Oscillations of Large Amplitude," *J. Acoust. Soc. Amer.*, **68**, 628 (1980).
Kirkwood, J. B., and H. A. Bethe, Office of Science Research and Development Rep. 558, Washington, DC (1942).
Lastman, G. J., and R. A. Wentzell, "Comparison of Five Models of Spherical Bubble Response in an Inviscid Compressible Liquid," *J. Acoust. Soc. Amer.*, **69**, 638 (1981).
Lauterborn, W., "Numerical Investigation of Non Linear Oscillations of Gas Bubbles in Liquids," *J. Acoust. Soc. Amer.*, **59**, 283 (1976).
Lauterborn, W., "Subharmonische Schwingungen von Gasblasen in Wasser," *Acustica*, (in German), **22**, 238 (1970).
Leighton, T. G., *The Acoustic Bubble*, Academic Press, San Diego, CA (1994).
Martin, P. D., and L. D. Ward, "Reactor Design for Sonochemical Engineering," *Chem. Eng. Res. Des.*, **70**, 296 (1992).
Martin, C. J., and A. N. R. Law, "The Use of Thermister Probes to Measure the Energy Distributions in the Bath," *Ultrasonics*, **18**, 127 (1980).
Martin, C. J., and A. N. R. Law, "The Use of Thermister Probes to Measure the Energy Distributions in the Bath," *Ultrasonics*, **21**, 85 (1983).
Mason, T. J., and J. P. Lorimer, *Sonochemistry: Theory, Applications and Uses of Ultrasound in Chemistry*, Horwood, New York (1988).
Matula, T. J., I. M. Hallaj, R. O. Cleveland, L. A. Crum, and R. A. Roy, "The Acoustic Emission from Single Bubble Sonoluminescence," *J. Acoust. Soc. Amer.*, **103**, 1377 (1998).
Naidu, D. V. P., R. Rajan, R. Kumar, K. S. Gandhi, V. H. Arakeri, and S. Chandrasekharan, "Modeling of Batch Sonochemical Reactor," *Chem. Eng. Sci.*, **49**, 877 (1994).
Nayfeh, A. S., and W. S. Saric, *Finite Amplitude Wave Effects in Fluids*, IPC Science and Technology Press, Guildford, CT (1974).
Neppiras, E. A., "Acoustic Cavitation," *Phys. Rep.*, **61**, 159 (1980).
Neppiras, E. A., "Subharmonic and Other Low Frequency Emission from Bubbles in Sound Irradiated Liquids," *J. Acoust. Soc. Amer.*, **46**, 587 (1969a).
Neppiras, E. A., "Subharmonic and Other Low Frequency Signals from Sound Irradiated Liquids," *J. Sound Vib.*, **10**, 176 (1969b).
Plesset, M. S., "Dynamics of Cavitating Bubbles," *J. Appl. Mech. Trans. ASME*, **16**, 277 (1949).
Plesset, M. S., and A. Prosperetti, "Bubble Dynamics and Cavitation," *Annu. Rev. Fluid Mech.*, **9**, 145 (1977).
Press, W. H., S. A. Teukolsky, and W. T. Vetterling, *Numerical Recipes*, Cambridge Univ. Press, Cambridge (1992).
Prosperetti, A., "Nonlinear Oscillations of Gas Bubbles in Liquids: Transient Solutions and the Connection Between Subharmonic Signal and Cavitation," *J. Acoust. Soc. Amer.*, **57**, 810 (1975).
Prosperetti, A., and K. W. Commander, "Linear Pressure Waves in

Bubbly Liquids: Comparison Between Theory and Experiment,'' *J. Acoust. Soc. Amer.*, **83**, 502 (1989).
Prosperetti, A., K. W. Commander, and L. A. Crum, ''Nonlinear Bubble Dynamics,'' *J. Acoust. Soc. Amer.*, **83**, 502 (1986).
Ratoarinoro, C., A. M. Wilhelm, and H. Delmas, ''Power Measurement in Sonochemistry,'' *Ultrason.-Sonochem.*, **2**, S43 (1995).
Rayleigh, L., ''On the Pressure Developed in a Liquid During the Collapse of Spherical Cavity,'' *Phil. Mag.*, **34**, 94 (1917).
Romdhane, M., A. Gadri, F. Contamine, C. Gourdon, and G. Casamatta, ''Experimental Study of the Ultrasound Attenuation in Chemical Reactors,'' *Ultrason.-Sonochem.*, **4**(3), 235 (1997).
Safar, M. H., ''Exploitation of the Subharmonic Pressure Waves from Pulsating Gas Bubbles in an Acoustic Field in Liquid,'' *J. Phys. D (Appl. Phys.)*, **3**, 635 (1970).
Walton, A. J., and G. T. Reynolds, ''Sonoluminescence,'' *Adv. Phys.*, **33**, 595 (1984).
Young, F. R., *Cavitation*, McGraw-Hill, London (1989).

*Manuscript received Mar. 8, 1999, and revision received Nov. 16, 1999.*